Journal of the Formosan Medical Association (2016) 115, 658–664

Available online at www.sciencedirect.com

ScienceDirect

journal homepage: www.jfma-online.com

ORIGINAL ARTICLE

A novel diagnostic method (spectral computed tomography of sacroiliac joints) for axial spondyloarthritis

Ping Zhang [a,b], Kai Hu Yu [c], Rui Min Guo [a], Jun Ran [a], Yao Liu [a], John Morelli [d], Val M. Runge [e], Xiao Ming Li [a,*]

[a] *Department of Radiology, Tongji Hospital, Tongji Medical College, Huazhong University of Science and Technology, Wuhan, Hubei, China*
[b] *Department of Radiology, Third Hospital of Hebei Medical University, Shijiazhuang, Hebei, China*
[c] *Department of Radiology, Xianning Central Hospital, Hubei University of Science and Technology, Xianning, China*
[d] *St John's Medical Center, Tulsa, OK, USA*
[e] *Institute of Diagnostic and Interventional Radiology, University Hospital Zurich, University of Zurich, Zurich, Switzerland*

Received 20 March 2015; received in revised form 27 June 2015; accepted 1 July 2015

KEYWORDS
axial spondyloarthritis;
sacroiliac joint;
spectral CT

Background/Purpose: To evaluate the diagnostic value of spectral computed tomography (CT) of sacroiliac joints for axial spondyloarthritis (SpA).
Methods: We retrospectively analyzed the records of 125 patients with low back pain (LBP) suspected of having SpA. Each patient underwent sacroiliac joint spectral CT examination. Water- and calcium-based material decomposition images were reconstructed. After 3–6 months of follow-up, 76 were diagnosed with SpA, and the remaining 49 patients were diagnosed with nonspecific LBP (nLBP). The slope of sacroiliac bone marrow HU (Hounsfield unit) curve (λ_{HU}), CT value, and bone marrow to normal muscle ratios of water and calcium concentrations in the ilium and sacrum were calculated and compared between nLBP and SpA patients.
Results: The iliac λ_{HU} was 8.26 ± 3.91 for nLBP and 9.81 ± 4.92 for SpA. The mean iliac ratios of water and calcium concentrations were 1.04 ± 0.03 and 21.67 ± 4.40, respectively, for nLBP, and 1.07 ± 0.04 and 111.5 ± 358.98, respectively, for SpA. The mean iliac CT values were 311.12 ± 86.52 HU for nLBP and 423.97 ± 127.51 HU for SpA. There were statistically significant differences in iliac ratios of water and calcium concentrations, CT value, and λ_{HU} between nLBP and SpA patients ($p < 0.05$). The sensitivity of iliac λ_{HU} was the highest. The diagnostic odds ratio of ratio of iliac calcium concentration was the highest, and its negative likelihood ratio was the lowest.

Conflicts of interest: The authors have no conflicts of interest relevant to this article.

* Corresponding author. Department of Radiology, Tongji Hospital, Tongji Medical College, Huazhong University of Science and Technology, Number 1095, Jiefang Road, Wuhan City 430030, Hubei Province, China.
E-mail address: lilyboston2002@163.com (X.M. Li).

http://dx.doi.org/10.1016/j.jfma.2015.07.003

Conclusion: Spectral CT not only shows bone erosion and sclerosis, but also shows and quantitatively measures bone marrow edema in the sacroiliac joints of SpA patients.

Introduction

Seronegative spondyloarthritis (SpA) is a chronic inflammatory rheumatologic disease. Sacroiliitis is the earliest clinical finding and is the diagnostic feature for SpA.[1] Computed tomography (CT) is sensitive in detecting the chronic changes in the sacroiliac joints (SIJs); however, magnetic resonance imaging (MRI) is more sensitive in identifying early signs of sacroiliitis including osteitis, enthesitis, and capsulitis.[2,3] With the increasing use of MRI to detect early features of SpA before identifiable radiographic features, the Assessment of Spondyloarthritis International Society (ASAS) has issued the updated criteria for the diagnosis of SpA. The presence of sacroiliitis is listed as one of the ASAS key criteria for the diagnosis of SpA.[4,5] As recommended by the ASAS criteria, the most commonly used MRI sequences for the assessment of SIJs are T1-weighted spin—echo sequences, and short tau inversion recovery (STIR) sequences.[6] Recently, the emergence of spectral CT has raised the possibility for measurements of relative water and calcium concentrations in bone via the acquisition of base material decomposition images. Spectral CT is performed by acquiring two consecutive scans with high and low energy (140 kV and 80 kV) using a single X-ray tube, a high-performance gemstone detector, and with implementation of powerful image postprocessing. By use of these techniques, accurate material decomposition images (i.e., water- and calcium-based material decomposition images) and monochromatic spectral images at energy levels ranging from 40 keV to 140 keV can be created.[7,8] The usefulness of spectral CT for musculoskeletal diseases in previous studies were primarily differential diagnosis of the osteoblastic metastases from bone islands in cancer patients, reduction of the metallic instrumentation artifacts, and detection of the uric acid depositing in tophaceous gout.[9—12] The aim of this study was to analyze whether the spectral CT sacroiliac imaging parameters could differentiate SpA and nLBP.

Methods

This study was approved by the Institutional Review Board of the Tongji hospital. Written informed consent was obtained from all participants.

Patient information

From October 2013 to May 2014, records of 125 patients (92 men and 33 women, age range 18—45 years, mean age 27.8 years) suffering from low back pain (LBP) lasting longer than 3 months and with clinical suspicion of SpA were retrospectively collected. All patients had experienced two or more of the following symptoms: insidious onset of pain/discomfort, morning stiffness, improvement of symptoms with exercise, or pain at night. None of the patients had histories of joint surgery, or intra-articular corticosteroid injections in the past 6 weeks, and none was treated with tumor necrosis factor α inhibitors or other biologic agents during the 3 months preceding the examination. Each patient underwent spectral CT and MRI examinations to evaluate the SIJs on the same day to reduce the influence of time factor in comparing the imaging finding of two methods. The spectral CT and MRI examinations were performed by the same radiologist who had $>$ 5 years of work experience.

After 3—6 months of follow-up, two fellowship-trained rheumatologists with $>$ 10 years of experience evaluated the presence of SpA based on the ASAS criteria.[4] According to ASAS criteria, a patient younger than 45 years with inflammatory back pain $>$ 3 months in duration can be diagnosed with SpA in the presence of (1) sacroiliitis on MRI or radiographic plus at least one typical clinical SpA feature or (2) the presence of positive-HLA-B27 plus at least two typical clinical SpA features. In these 125 patients, 76 patients (17 women, 59 men, age range 18—43 years, mean age 26.4 years) were diagnosed with SpA, and 49 patients (14 women, 35 men, age range 18—44 years, mean age 29.3 years) were diagnosed with nonspecific LBP (nLBP).

Equipment and scanning techniques

All CT scans were obtained using a standard spectral CT scanner (GE Discovery 750 high-definition CT; GE Healthcare, Milwaukee, WI, USA), and MRIs were performed using a 1.5-T MRI scanner (Signa HDxt; GE Healthcare).

The spectral CT scanning parameters were as follows: collimation thickness, 0.625 mm; tube current, 550 mA; rotation speed, 0.8 second; helical pitch, 0.984. Two types of images were reconstructed from the single spectral CT acquisition: conventional polychromatic images obtained at 140 kVp and monochromatic images obtained at energy of 70 keV. Slice thickness and spacing were 0.625 mm and 0.625 mm, respectively.

The MRI scanning sequences were as follows: (1) an axial fast spin echo sequence [repetition time/echo time (TR/TE) = 280/7.2 ms, slice thickness = 4 mm]; (2) an axial fast recovery fast spin—echo sequence with fat suppression (TR/TE = 2220/86 ms, slice thickness = 4 mm); and (3) an oblique coronal STIR sequence (TR/TE = 4100/71.2 ms, inversion time [TI] = 150 ms, slice thickness = 4 mm).

Image analysis and diagnosing criteria

Two musculoskeletal radiologists with $>$ 5 years of musculoskeletal imaging experience, blinded to the diagnosis and

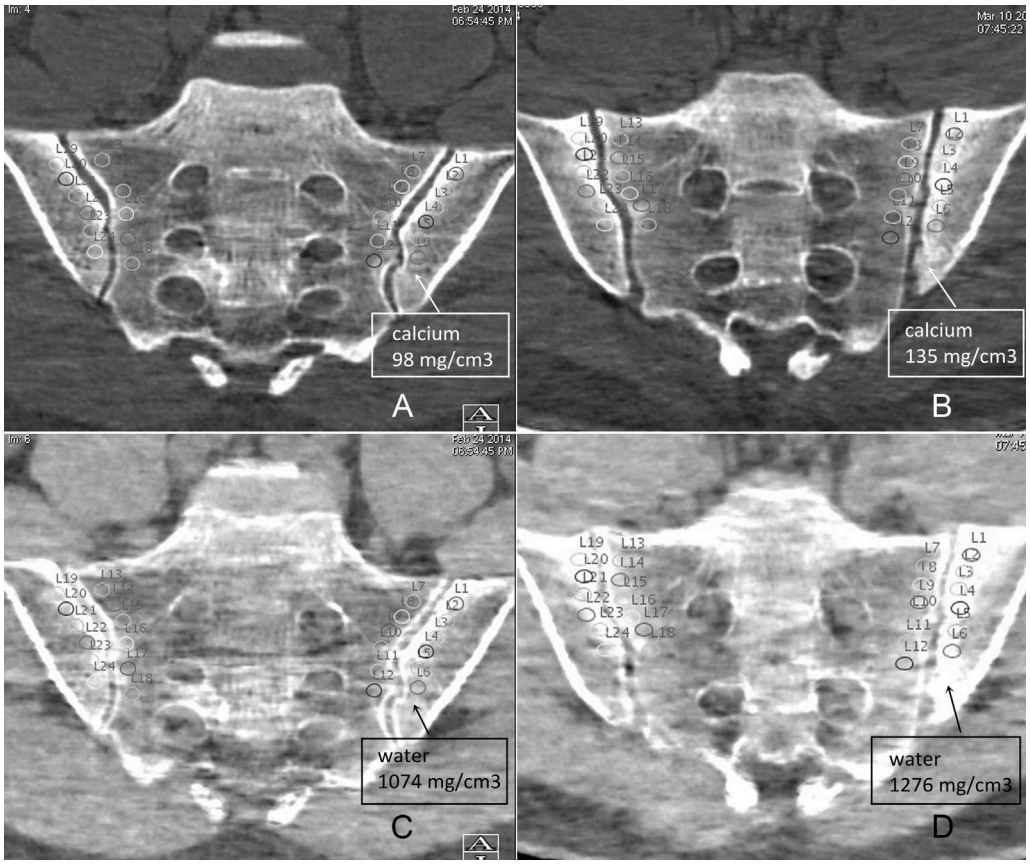

Figure 1 (A,C) A patient with nLBP (male, 22 years old, HLA-B27 negative, low back pain for 3 months); (B,D) A patient with SpA (male, 20 years old, HLA-B27 positive, low back pain for 3 months). The relative calcium concentration images (A,B) show the mean calcium concentration of left ilium of the SpA patient (135 mg/cm^3) is higher than that of nLBP patient (98 mg/cm^3). Similarly, the relative water concentration images (C,D) show that the mean water concentration of the left ilium of the SpA patient (1276 mg/cm^3) was higher than that of the nLBP patient (1074 mg/cm^3). nLBP = nonspecific low back pain; SpA = spondyloarthritis.

patient demographics, evaluated all spectral CT and MRI images, respectively. Features evaluated by the readers included the presence or absence of: bone marrow edema, bone sclerosis, bone cortex erosion, and SIJ space narrowing. On the water base material decomposition images of spectral CT, when the subcortical bones of the SIJs presented high density (the water concentration was increased), there was bone marrow edema in subcortical bones.

Image postprocessing and data collection

The monochromatic images were analyzed by a dedicated workstation of Gemstone Spectral CT Imaging (GSI) viewer (AW 461; GE Healthcare). Through GSI reconstruction, base material decomposition images were made choosing calcium and water as the base materials. In the oblique coronal plane of the SIJ, six circular regions of interest (ROIs; 19—21 mm^2) were semiautomatically placed separately in the subcortical bones of the SIJs bilaterally. The distance between the center of the ROI and the bone cortex ranged from 4 mm to 6 mm, to avoid the influence of the cortex in the analysis (Figure 1). Within the same image slice, two ROIs (about 30 mm^2) were respectively placed in normal psoas major muscles. The ratios of marrow water and calcium concentration to muscle water and calcium concentration were calculated. The polychromatic images were transmitted to the same workstation to reconstruct the oblique coronal images. ROIs were drawn analogously to measure the CT values [Hounsfield unit (HU)] of both subcortical sacral and iliac regions.

Quantitative parameters included the following: (1) the ratio of water concentrations; (2) the ratio of calcium

Table 1 Comparison of imaging findings of spectral CT and MRI.

Methods	Bone marrow edema	Bone sclerosis	Bone cortex erosion	Sacroiliac joint space narrowing
Spectral CT	56/76	60/76	65/76	8/76
MRI	53/76	47/76	47/76	8/76

CT = computed tomography; MRI = magnetic resonance imaging.

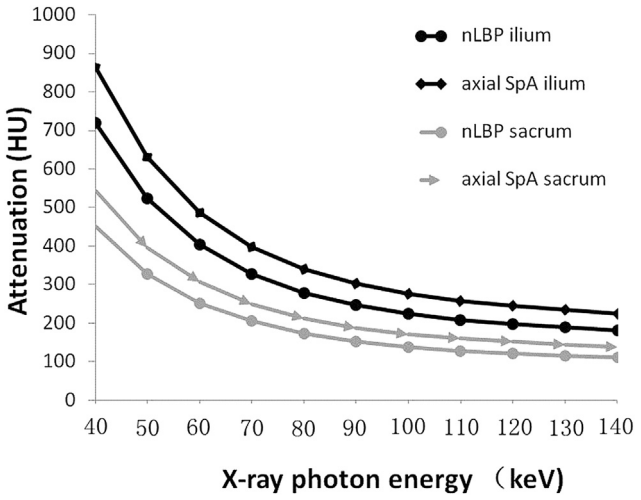

Figure 2 Attenuation to X-ray photon energies curves (HU curves) corresponding to subcortical bones of SIJs in patients with nLBP and SpA. HU = Hounsfield unit; nLBP = nonspecific low back pain; SIJs = sacroiliac joints; SpA = spondyloarthritis.

concentration; (3) the slope of HU curves (λ_{HU}; the plot of material attenuation against X-ray photon energy) corresponding to subcortical sacrum and ilium calculated as the CT attenuation difference at two energy levels (40 keV and 100 keV) divided by the energy difference (60 keV) from the HU curve:

$$\lambda_{HU} = (HU_{40keV} - HU_{100keV})/60; \quad (1)$$

and (4) CT values (HU) of bilateral subcortical sacrum and ilium in polychromatic images. The two musculoskeletal radiologists, blinded to the diagnosis and patient characteristics, independently measured the quantitative parameters in sacra and ilia.

Data analysis

The data were analyzed using SPSS version 17.0 for Windows (SPSS Inc., Chicago, IL, USA). Continuous variables were described as mean ± standard deviations. A paired sample *t* test was used to analyze the differences of parameters (water concentration, calcium concentration, and CT value) between the left and right sides of the SIJ. If there were no statistical differences in the parameters between the left and right sides, the mean value was the total of 12 ROIs. An independent sample *t* test was used to analyze the differences of parameters between nLBP and SpA groups. Receiver operating characteristic curves were constructed to evaluate the sensitivity and specificity of parameters in identifying SpA and nLBP patients. The cutoff value was chosen as the point maximizing Youden's index. A p value < 0.05 was considered statistically significant.

Results

No statistically significant differences were identified between the SpA and nLBP patients with respect to age and sex. Seventy-three (96.1%) patients with SpA were HLA-B27 positive, whereas 14 (28.6%) patients with nLBP were HLA-B27 positive.

In 76 patients with SpA, 53 (69.7%) patients had bone marrow edema on both spectral CT and MRI. Three (3.9%) patients had bone marrow edema on spectral CT but no suspicious findings on MRI. Meanwhile, 47 (61.8%) patients had bone sclerosis on both spectral CT and MRI. Thirteen (17.1%) patients had bone sclerosis on spectral CT but no findings on MRI. Forty-seven (61.8%) patients had bone cortex erosions identified on both spectral CT and MRI. Eighteen (23.7%) patients had bone cortex erosions on spectral CT but no findings on MRI. Eight (10.5%) patients had SIJ space narrowing on both spectral CT and MRI (Table 1).

Attenuation to X-ray photon energy curves (HU curves) corresponding to the subcortical bones of SIJs in patients with nLBP and SpA are shown in Figure 2. A quantitative analysis of the HU curves showed positive λ_{HU} for the nLBP group (5.24 ± 3.11 and 8.26 ± 3.91) and the axial SpA group (6.23 ± 4.23 and 9.81 ± 4.92), respectively, in the sacrum and the ilium. There were statistically significant differences of λ_{HU} between nLBP and SpA groups in the sacrum ($t = -4.83$, $p < 0.001$) and in the ilium ($t = -6.36$, $p < 0.001$).

There was no statistical difference in water concentration, calcium concentration, and CT value between the left

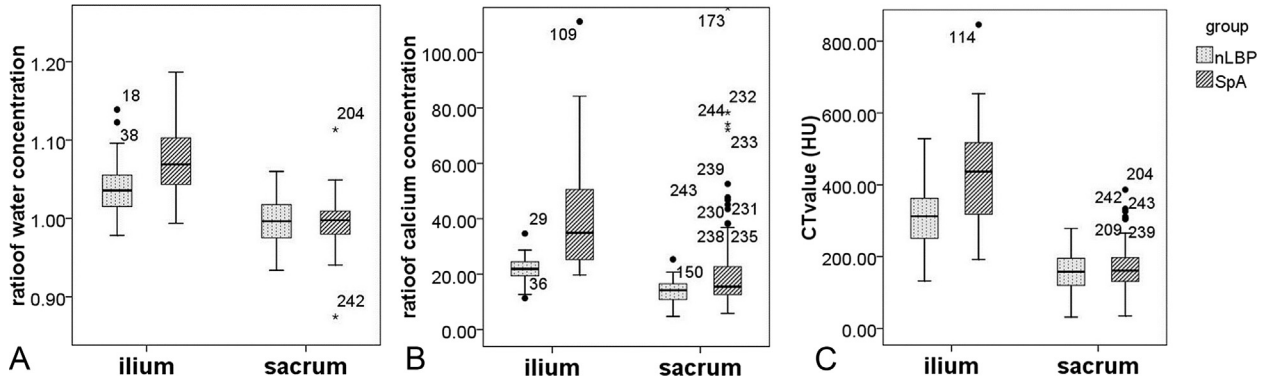

Figure 3 Box plots demonstrating statistically significant differences in (A) ratio of water concentrations, (B) ratio of calcium concentrations, and (C) computed tomography (CT) values in ilium.

Table 2 Statistical results of spectral CT parameters.

Parameters	Group	Mean	SD	*t*	*p*
Iliac ratio of water concentration	nLBP	1.04	0.03	−5.10	0.000
	SpA	1.07	0.04		
Sacral ratio of water concentration	nLBP	1.00	0.03	0.062	0.951
	SpA	1.00	0.03		
Iliac ratio of calcium concentration	nLBP	21.67	4.40	−2.17	0.033
	SpA	111.15	358.98		
Sacral ratio of calcium concentration	nLBP	13.76	4.09	−1.99	0.051
	SpA	44.54	135.08		
Iliac CT value (HU)	nLBP	311.12	86.52	−5.89	0.000
	SpA	423.97	127.51		
Sacral CT value (HU)	nLBP	162.43	57.01	−0.69	0.494
	SpA	170.17	64.40		

CT = computed tomography; HU = Hounsfield unit; nLBP = nonspecific low back pain; SD = standard deviation; SpA = spondyloarthritis.

and right sides of the sacrum and the ilium ($p > 0.05$). The mean iliac ratios of water and calcium concentrations were 1.04 ± 0.03 and 21.67 ± 4.40, respectively, for nLBP patients, and 1.07 ± 0.04 and 111.5 ± 358.98, respectively, for SpA patients. The mean iliac CT values were 311.12 ± 86.52 HU for nLBP patients and 423.97 ± 127.51 HU for SpA patients. There were statistically significant differences (Figure 3) in ratio of water concentration ($t = -5.10$, $p < 0.05$), ratio of calcium concentration ($t = -2.17$, $p < 0.05$), and CT value ($t = -5.89$, $p < 0.05$) between nLBP and SpA patients in the ilia (Table 2).

To assess the capability of the iliac ratio of water and calcium concentrations, CT value, and slope of the HU curve in detecting SpA patients, receiver operating characteristic curves were constructed and areas under the curve (AUCs) were computed (Figure 4). The iliac parameters of AUC, cutoff value, sensitivity, specificity, positive likelihood ratio, negative likelihood ratio, and diagnostic odds ratio are shown in Table 3. The cutoff values of iliac ratio of water concentration, calcium concentrations, CT value, and slope of HU curve were 1.05, 27.73, 378.81 HU, and 8.04, respectively. The diagnostic sensitivity of the slope of the HU curve (75%) was the highest, whereas its diagnostic specificity (57.1%) was the lowest. The diagnostic specificity of the ratio of calcium concentration (95.9%) was the highest. The positive likelihood ratio of the ratio of calcium concentration was the highest (16.05), its diagnostic odds ratio (44.58) was the highest, its AUC was the largest, and its negative likelihood ratio (0.36) was the lowest.

Discussion

Subcortical bone marrow edema is an important feature of active SpA. Normal peripheral bone marrow is filled with adipocytes, whereas an edematous cancellous bone is characterized by an accumulation of immune cells and microvasculature in the bone marrow replacing the marrow adipocytes. This leads to an increase in water content and a decrease in fat content.[13] MRI demonstrating periarticular SIJ bone marrow edema is considered to be the imaging hallmark of SpA.[14] In this study, the mean iliac ratio of water and calcium concentrations of SpA patients as calculated on spectral CT were higher than those of the nLBP patients. When the ratios of water and calcium concentrations and CT values were used to detect sacroiliitis in axial SpA patients, the sensitivity of the ratio of water concentration was 69.7%. Additionally, three (3.9%) patients with SpA had bone marrow edema on spectral CT but without associated findings on MRI. This may relate to the low signal/noise ratios of the MRIs,[15] which may prevent the detection of subtle bone marrow edema. The STIR or fat-suppressed T2-weighted images are sensitive to the presence of free water, but the normal peripheral bone marrow contains adipocytes and fat-rich compartment.

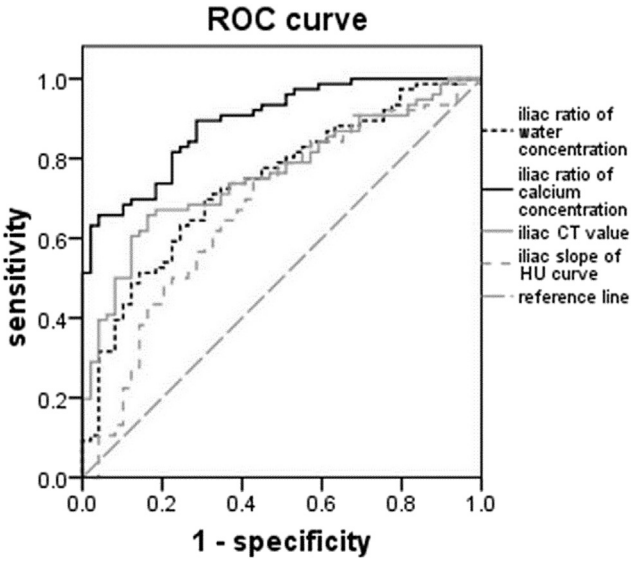

Figure 4 ROC curves for iliac ratio of water concentration, iliac ratio of calcium concentration, iliac CT value, and iliac slope of HU curve in differentiating SpA patients from nLBP patients. CT = computed tomography; HU = Hounsfield unit; nLBP = nonspecific low back pain; ROC = receiver operating characteristic; SpA = spondyloarthritis.

Table 3 Diagnosis performance indices of iliac spectral CT parameters.

Iliac parameters	Ratio of water concentration	Ratio of calcium concentration	CT value	Slope of HU curve
AUC	0.740	0.892	0.760	0.676
Cutoff value	1.05	27.73	378.81	8.04
Sensitivity (%)	69.7	65.8	65.8	75.0
Specificity (%)	69.4	95.9	83.7	57.1
Positive likelihood ratio	2.28	16.05	4.04	1.75
Negative likelihood ratio	0.44	0.36	0.41	0.44
Diagnostic odds ratio	5.18	44.58	9.85	4.00

AUC = area under the curve; CT = computed tomography; HU = Hounsfield unit.

STIR images may suppress the signal of water protons bound to proteins with a T1 similar to that of fat.[15,16] Spectral CT could show bone marrow edema in the osteosclerotic part of the bone, whereas the STIR images remain insensitive in this regard. When patients are with a birth control ring or metallic implantation, or have intolerance to long time examination, spectral CT is a reliable method for SpA diagnosis. Additionally, in this study, 13 (17.1%) patients had bone sclerosis on spectral CT but had no corresponding findings on MRI. Eighteen (23.7%) patients had bone cortex erosions on spectral CT but had no such findings on MRI. Spectral CT could detect the small bone erosions and slight bone sclerosis. What is more, it could also quantitatively measure bone marrow edema and bone sclerosis in the SIJs of SpA patients.

In all of the diagnosis performance indices of iliac spectral CT parameters (Table 3), the sensitivity of the slope of the HU curve is the highest, but its specificity is also the lowest. That is to say, the misdiagnosis rate is high when one is using the slope of the HU curve as the only diagnosis index. The positive likelihood ratio (the ratio of true positive rate and false positive rate) of the ratio of calcium concentration is the highest. The positive likelihood ratio is not influenced by disease prevalence and is the common concern among clinicians. The diagnostic odds ratio of rate of calcium concentration is the highest—that is to say, this index has the highest ability to distinguish SpA and nLBP.

In this study, the histological structures of sacra and ilia in nLBP and SpA patients were the bone tissues, so the attenuation to X-ray photon energy curves (Figure 2) were observed to steadily decrease with higher energy levels. Because the component contents (calcium, water, fat, etc.) of sacra and ilia were different between nLBP and SpA patients, the slope of HU curves were significantly different between the nLBP and SpA groups.

The ratio of water and calcium concentrations of SpA patients were both higher than those of nLBP patients in the ilium. This may be related with the chronic inflammation and inflammatory infiltration in the SIJ. The proinflammatory cytokines stimulate the osteoclast differentiation and function.[17] Meanwhile, the serum osteoprotegerin levels were increased to regulate bone resorption by inhibiting osteoclast differentiation and activation and inducing osteoclast apoptosis.[18]

In patients with SpA, iliac ratio of calcium and water concentrations increased more dramatically than these values on the sacral side of the SIJ. This finding confirms the results of previous studies in early ankylosing spondylitis patients that found the ilium to be involved earlier in the disease process than the sacrum.[19,20] There are several proposed mechanisms for this. For one, the cartilage on the ilial side (0.8 mm) is thinner than that on the sacral side (1.8 mm).[21] Moreover, iliac cartilage is by a mixture of hyaline and fibrocartilage, whereas the sacral cartilage is purely hyaline.[22] It may thus target the interface between the bone and fibrocartilage,[23] similar to the hypothesized mechanism for enthesitis. Finally, distribution of weight-bearing forces may differ between the sides of the SIJs,[24] thus contributing to the differential onset of inflammation between the sacral and iliac sides of the SIJ.

The initial velocity (velocity of X-ray converting to visible light) of spectral CT is faster than that of conventional CT by about 100 times, and the emptying rate (afterglow effect) is faster than that of conventional CT by about four times. So, the radiation dose of spectral CT is lower than that of conventional CT.

This study has several limitations. First, there was a selection bias in the retrospective study. Second, this study lacks SIJ degeneration or osteitis condensans ilii cases, whose clinical symptoms are similar to those of SpA. In future studies, it may also be useful to assess the differences in the ratio of water and calcium concentrations in these groups. Third, further study may be needed to correlate the findings of spectral CT imaging with those of MRI for the differential diagnosis of sacroiliitis in patients with and without SpA.

Conclusion

Spectral CT not only shows bone erosion and sclerosis, but may also show and quantitatively measure bone marrow edema in the SIJs of SpA patients.

Acknowledgments

This research was supported by the projects from National Scientific foundation of China (Numbers: 81320108013 and 31170899).

References

1. Brandt J, Bollow M, Haberle J, Rudwaleit M, Eqqens U, Distler A, et al. Studying patients with inflammatory back pain

and arthritis of the lower limbs clinically and by magnetic resonance imaging: many, but not all patients with sacroiliitis have spondyloarthropathy. *Rheumatology* 1999;**38**:831—6.
2. Braun J, Sieper J, Bollow M. Imaging of sacroiliitis. *Clin Rheumatol* 2000;**19**:51—7.
3. Braun J, Golder W, Bollow M, Sieper J, van der Heijde D. Imaging and scoring in ankylosing spondylitis. *Clin Exp Rheumatol* 2002;**20**:S178—84.
4. Rudwaleit M, van der Heijde D, Landewe R, Listing J, Akkoc N, Brandt J, et al. The development of Assessment of SpondyloArthritis international Society classification criteria for axial spondyloarthritis (part II): validation and final selection. *Ann Rheum Dis* 2009;**68**:777—83.
5. Rudwaleit M, Landewe R, van der Heijde D, Listing J, Brandt J, Braun J, et al. The development of Assessment of SpondyloArthritis international Society classification criteria for axial spondyloarthritis (part I): classification of paper patients by expert opinion including uncertainty appraisal. *Ann Rheum Dis* 2009;**68**:770—6.
6. Rudwaleit M, Jurik AG, Hermann KG, Landewe R, van der Heijde D, Baraliakos X, et al. Defining active sacroiliitis on magnetic resonance imaging (MRI) for classification of axial spondyloarthritis: a consensual approach by the ASAS/OMERACT MRI group. *Ann Rheum Dis* 2009;**68**:1520—7.
7. Wang L, Liu B, Wu XW, Wang J, Zhou Y, Wang WQ, et al. Correlation between CT attenuation value and iodine concentration in vitro: discrepancy between gemstone spectral imaging on single-source dual-energy CT and traditional polychromatic X-ray imaging. *J Med Imaging Radiat Oncol* 2012;**56**:379—83.
8. Lv P, Lin XZ, Li J, Li W, Chen K. Differentiation of small hepatic hemangioma from small hepatocellular carcinoma: recently introduced spectral CT method. *Radiology* 2011;**259**:720—9.
9. Li X, Wang X, Yu Y, Liu B, Cai J, Xia L, et al. Detection of uric acid depositing in tophaceous gout using a new dual energy spectral CT technology. *J X-ray Sci Technol* 2014;**22**:541—9.
10. Zheng S, Dong Y, Miao Y, Liu A, Zhang X, Wang B, et al. Differentiation of osteolytic metastases and Schmorl's nodes in cancer patients using dual-energy CT: advantage of spectral CT imaging. *Eur J Radiol* 2014;**83**:1216—21.
11. Dong Y, Zheng S, Machida H, Wang B, Liu A, Liu Y, et al. Differential diagnosis of osteoblastic metastases from bone islands in patients with lung cancer by single-source dual-energy CT: advantages of spectral CT imaging. *Eur J Radiol* 2015;**84**:901—7.
12. Komlosi P, Grady D, Smith JS, Shaffrey CI, Goode AR, Judy PG, et al. Evaluation of monoenergetic imaging to reduce metallic instrumentation artifacts in computed tomography of the cervical spine. *J Neurosurg Spine* 2015;**22**:34—8.
13. Schett G. Bone marrow edema. *Ann N Y Acad Sci* 2009;**1154**:35—40.
14. Slobodin G, Rosner I. Indemonstrable axial spondyloarthritis: does it exist? *Isr Med Assoc J* 2013;**15**:780—1.
15. Del Grande F, Santini F, Herzka DA, Aro MR, Dean CW, Gold GE, et al. Fat-suppression techniques for 3-T MR imaging of the musculoskeletal system. *Radiographics* 2014;**34**:217—33.
16. Krinsky G, Rofsky NM, Weinreb JC. Nonspecificity of short inversion time inversion recovery (STIR) as a technique of fat suppression: pitfalls in image interpretation. *AJR Am J Roentgenol* 1996;**166**:523—6.
17. Baum R, Gravallese EM. Impact of inflammation on the osteoblast in rheumatic diseases. *Curr Osteoporos Rep* 2014;**12**:9—16.
18. Chen CH, Chen HA, Liao HT, Liu CH, Tsai CY, Chou CT. Soluble receptor activator of nuclear factor-kappaB ligand (RANKL) and osteoprotegerin in ankylosing spondylitis: OPG is associated with poor physical mobility and reflects systemic inflammation. *Clin Rheumatol* 2010;**29**:1155—61.
19. Carlson GC, Shipley MT, Keller A. Long-lasting depolarizations in mitral cells of the rat olfactory bulb. *J Neurosci* 2000;**20**:2011—21.
20. Muche B, Bollow M, Francois RJ, Sieper J, Hamm B, Braun J. Anatomic structures involved in early- and late-stage sacroiliitis in spondylarthritis: a detailed analysis by contrast-enhanced magnetic resonance imaging. *Arthritis Rheum* 2003;**48**:1374—84.
21. McLauchlan GJ, Gardner DL. Sacral and iliac articular cartilage thickness and cellularity: relationship to subchondral bone end-plate thickness and cancellous bone density. *Rheumatology* 2002;**41**:375—80.
22. Benjamin M, McGonagle D. The anatomical basis for disease localisation in seronegative spondyloarthropathy at entheses and related sites. *J Anat* 2001;**199**:503—26.
23. Maksymowych WP. Ankylosing spondylitis—at the interface of bone and cartilage. *J Rheumatol* 2000;**27**:2295—301.
24. de Bosset P, Gordon DA, Smythe HA, Urowitz MB, Koehler BE, Singal DP. Comparison of osteitis condensans ilii and ankylosing spondylitis in female patients: clinical, radiological and HLA typing characteristics. *J Chronic Dis* 1978;**31**:171—81.